Geoderma 442 (2024) 116770

Contents lists available at ScienceDirect

Geoderma

journal homepage: www.elsevier.com/locate/geoderma

Optimized measurement of frozen soil thermal properties using a heat-pulse sensor

Tianyue Zhao [a,1], Yuanyuan Zhang [a,1], Hailong He [b], Robert Horton [c], Gang Liu [a,*]

[a] Department of Land Use Engineering, College of Land Science and Technology, China Agricultural University, Beijing 100193, China
[b] College of Natural Resources and Environment, Northwest A&F University, Yangling 712100, China
[c] Department of Agronomy, Iowa State Univ., Ames, IA 50011, USA

ARTICLE INFO

Handling Editor: L. Morgan Cristine

Keywords:
Frozen soils
Dual probe Heat pulse method
Finite element simulation
Heat conduction equation
Analytical solution

ABSTRACT

The measurement of thermal properties in partially frozen soil is crucial for global climate models. As the primary method for soil thermal property measurement, the Dual-Probe Heat-Pulse (DPHP) sensor experiences significant errors when used in partially frozen soils. The application of heat pulses leads to ice melting, and the existing DPHP theory, which does not consider phase changes, fails to accurately determine thermal conductivity (k) and heat capacity (C) in the temperature range of − 5 °C to 0 °C. There is a lack of DPHP theory specifically designed for use in partially frozen soils. The existing DPHP theory employs the Infinite Linear Source (ILS) approximation, which does not account for the melting process and the moving ice-liquid interface in transient heat conduction theory. Currently, there is no effective and reliable method to assess DPHP errors associated with measuring the thermal properties of partially frozen soil. To accurately determine k and C in frozen soil, it is essential to perform an error analysis regarding ice melting caused by a DPHP heat pulse input. In this study, (1) we considered the latent heat of ice melting and a moving ice-liquid interface in finite element simulations and compared the results with an analytical solution presented by Paterson (1952); (2) we performed simulations of DPHP measurements based on the temperature-dependent ice content, liquid water content, and melting latent heat of three frozen soils used by Watanabe and Wake (2009); (3) based on COMSOL simulation results for the three frozen soils, we determined the optimal heating parameter combinations (heating duration, t_0, and accumulated heating energy, ΔQ) to minimize DPHP measurement errors in frozen soil. The results showed that (1) Simulations that included the melting phase changes were in agreement with the analytical solution by Paterson (1952). (2) Including the ice-liquid moving interface significantly altered the spatial distribution characteristics of temperature, which were not captured by the ILS model in terms of the temperature distribution near the interface. (3) Below a temperature of − 5.5 °C, the simulations that included phase changes were consistent with measured results; (4) For partially frozen soils with initial temperatures ranging from − 0.5 °C to 0 °C, the relative errors in thermal conductivity fitted by the ILS model exceeded 100 %. To mitigate the influence of ice melting, we recommend using $200 < \Delta Q < 400$ J m^{-1} for sand, loam, and silt loam soils with 8 s < t_0 < 60 s. For a loam soil with $t_0 = 60$ s, $\Delta Q = 800$ J m^{-1} should be used. For a silt loam soil with $t_0 = 60$ s, we recommend using $\Delta Q = 600$ J m^{-1}. If the ILS model is chosen to calculate soil thermal properties, we recommend using $200 < \Delta Q < 600$ J m^{-1} and 30 s < t_0 < 60 s for sandy and silt loam soils. For a loam soil, we recommend using $400 < \Delta Q < 800$ J m^{-1} and 30 s < t_0 < 60 s.

1. Introduction

Soil thermal properties are important parameters for calculating surface temperature, estimating surface energy balance, studying soil heat transfer coefficients, and investigating freeze–thaw depth (Orakoglu Firat et al., 2021; He et al., 2020). Partially frozen soil is a complex composite consisting of soil particles, air, ice, and unfrozen water. The freezing and thawing processes of soil lead to pore deformation and changes in the soil skeletal structure (Mustamo et al., 2019; Rooney et al., 2022). Additionally, the coexistence of liquid water and

* Corresponding author.
E-mail address: liug@cau.edu.cn (G. Liu).
[1] These authors contributed to the work equally and should be regarded as co-first authors.

https://doi.org/10.1016/j.geoderma.2023.116770
Received 21 September 2023; Received in revised form 20 December 2023; Accepted 29 December 2023
Available online 12 January 2024

ice can lead to soil frost heave and shrinkage, resulting in spatial heterogeneity of soil physical properties (Cuo et al., 2023). These factors pose significant challenges to accurately measure and simulate the thermal properties of partially frozen soil, particularly when the soil temperature is slightly below 0 °C (Jiao et al., 2022; Zhao et al., 2018; Zhao et al., 2019), and the presence of melting further increases measurement errors in thermal properties.

In recent years, the Dual-Probe Heat-Pulse sensor (DPHP) has been used to measure thermal properties of frozen soil (Kojima et al., 2018; Putkonen et al., 2003), ice content (He et al., 2015; Liu et al., 2011; Tian et al., 2015), and snow density (Liu and Si, 2008). However, a heat pulse causes soil ice to melt, violating the theoretical foundation of the existing DPHP method (heat conduction without a phase change), rendering inaccurate DPHP thermal property measurements (Liu and Si, 2011; Ochsner et al., 2008). To date, this issue remains unresolved. Putkonen et al. (2003) demonstrated that a DPHP is not suitable to measure thermal properties of frozen soil in the temperature range of − 10 °C to 0 °C. The results of Kojima et al. (2016) showed that a DPHP overestimates the thermal conductivity (k) of frozen soil in the range of − 2 °C to 0 °C. He et al. (2015) studied a sandy soil with a total water content of 0.25 m^3 m^{-3} and found that ice melting induced by a DPHP primarily occurred in the temperature range of − 1.5 °C to − 0.5 °C. Some investigators reported that a DPHP could accurately measure the heat capacity of frozen soil at temperatures below − 5 °C but not in the range of − 2 °C to 0 °C (Tian et al., 2015; Zhang et al., 2011). Although these measurements confine the temperature range for making accurate DPHP measurements in frozen soil, they do not consider latent heat of phase changes and the existence of a moving solid–liquid interface (Liu and Si, 2011; Zhang et al., 2011), making it difficult to assess the accuracy and reliability of the measurements.

Existing theories used to study frozen soil thermal properties, such as the Infinite Line Source (ILS) model, rely on single-phase heat transfer approximations and neglect the coexistence of ice and water. This leads to a mismatch between theoretical predictions and actual processes (Ochsner and Baker, 2008). Simulations and measurements both fail to provide accurate and reliable reference values. Although there can be large measurement errors in DPHP determined frozen soil thermal property values (Liu and Si, 2011; Zhang et al., 2011), an effective method to reduce this error is lacking. In order to improve the measurement accuracy of frozen soil thermal properties, some investigators have used apparent thermal properties (approximating the latent heat of phase transition with apparent heat capacity) instead of relying on actual soil thermal property values (He et al., 2015; Kojima et al., 2014; Zhao et al., 2019). This approach essentially treats the problem as a stable medium heat transfer issue and does not provide the interface location of the melting phase transition. Due to the lack of comparison with more rigorous theories and simulation results considering ice-liquid two-phase moving interfaces, the effectiveness and error of using apparent heat capacity as an approximation are unknown.

Although heat transfer theories considering ice-liquid phase transitions have been proposed (Paterson, 1952; Hahn et al., 2012) and provide analytical expressions for the temperature distribution in ice-liquid phases, there have been no reports on the application of these theories to frozen soils. The method of Paterson (1952) is only applicable to the case where thermal properties do not vary with temperature. The nonlinear temperature-dependent thermal properties of actual frozen soil lead to the evolution of a nonlinear partial differential equation for heat conduction. Currently, mathematical methods lack the ability to solve the nonlinear equations analytically (Arfken and Weber, 2005). Thus, numerical computations are used to solve the nonlinear heat conduction equation.

Numerical simulation methods have been used to study heat transfer processes in frozen soil. Zhang et al. (2011) simulated DPHP measurements of frozen soil thermal properties using a Finite Difference Numerical Method (FDNM), but they only considered the latent heat of phase transition without distinguishing between ice and liquid interfaces. Moreover, their simulation results deviated significantly from measured values when the soil temperature was between − 2 °C and 0 °C. Although Bao et al. (2016) incorporated latent heat in their frozen soil model, they neglected a moving ice-liquid interface. Finite element simulations have been extensively applied in soil physics research (Liu et al., 2006; Liu et al., 2016; Sang et al., 2020). However, to date, there are no reports of finite element simulations that simultaneously consider the latent heat of phase transition and ice-liquid interfaces for DPHP studies in frozen soil.

Numerical simulations can be used to complement experiments. In addition to the issue of ice-liquid interfaces during melting, there are several sources of error in DPHP measurements that affect measurement accuracy. For instance, during the freeze–thaw process, the expansion of ice in frozen soil can exacerbate measurement errors caused by changes in sensor probe spacing. Probe spacing is a crucial and sensitive parameter in DPHP measurements (Kluitenberg et al., 1993), and Liu et al. (2008) demonstrated that a 1° angular deviation in the probe can result in relative errors greater than 10 % in specific heat and thermal diffusivity. By using numerical simulations, these types of measurement errors can be effectively avoided, (1) disturbances from unknown environmental factors, such as non-uniform soil structure, soil moisture distribution, non-uniform temperature fields (Jury and Bellantuoni, 1976), and solar radiation fluctuations (Sang et al., 2021), which can all affect frozen soil near 0 °C; (2) changes in probe spacing during freeze–thaw cycles (Kluitenberg et al., 1993; Liu et al., 2008); (3) contact thermal resistance between the probe and soil (Liu and Si, 2010); (4) background temperature fluctuations, wind speed (Sang et al., 2020; Sang et al., 2021), and soil spatial heterogeneity. Using computer simulations, numerous factors that influence the measurement of frozen soil thermal properties (such as soil spatial heterogeneity, non-uniform soil temperature field distributions, environmental temperature fluctuations) can be systematically isolated in order to identify ways to optimize DPHP measurement results. Furthermore, unlike physical DPHP experiments, computer simulations require the pre-specification of frozen soil thermal properties, making the soil thermal properties known and enabling an accurate evaluation of DPHP errors under various conditions. To the best of our knowledge, current DPHP simulations for frozen soil thermal properties have not considered ice-liquid interfaces.

In this study, we use the analytical solution of Paterson (1952) to consider ice-liquid interfaces and latent heat of phase changes during DPHP measurements. We also use finite element methods to investigate the sources of error and influencing factors in measuring frozen soil thermal properties using DPHP. Our primarily research objectives include: (1) comparing the predicted results of the Paterson (1952) analytical solution which considers latent heat of phase transition and ice-liquid interfaces with the results of the ILS model that does not consider phase change; (2) verifying the feasibility of simulating frozen soil DPHP measurements with COMSOL; (3) simulating the Watanabe et al. (2009) DPHP measurements on frozen soil within the temperature range of − 5 °C to 0 °C, addressing the errors of the DPHP method in these measurements, and discovering the combinations of heating intensity and duration that minimize the errors.

2. Materials and Methods

2.1. Analytical Solution for a DPHP Measurement without Considering Melting Phase changes (Cylindrical Coordinate System)

The Infinite Line Source (ILS) is a mainstream DPHP model (De Vries, 1952; Kluitenberg et al., 1995). Temperature changes following the initiation of a heat pulse input are described by the following equation:

$$\Delta T(r,t) = \begin{cases} -\frac{q'}{4\pi k} Ei\left(\frac{-r^2}{4\alpha t}\right) & 0 < t < t_0 \\ -\frac{q'}{4\pi k}\left\{Ei\left[\frac{-r^2}{4\alpha(t-t_0)}\right] - Ei\left(\frac{-r^2}{4\alpha t}\right)\right\} & t > t_0 \end{cases} \quad (1)$$

where $-Ei(-x)$ represents the exponential integral, t denotes time (s), t_0 represents the duration of heating (s), q' is the heating intensity (W m^{-1}), and r is the distance from the line heat source (m). By using the nonlinear fitting function of Mathematica 12.1 (Wolfram Research, Inc., Champaign, IL), the temperature response curve obtained from heat pulse probe measurements (Equation (1)) can be used to determine the thermal conductivity k (W m^{-1} K^{-1}), thermal diffusivity α (m^2 s^{-1}), and volumetric heat capacity of the soil C ($C = k/\alpha$, J m^{-3} K^{-1}). The ILS model considers only single medium heat conduction and does not account for melting phase transitions. From Equation (1), it is clear that this model does not differentiate between solid (ice) and liquid phases.

2.2. Theory for Frozen Soil Heat Conduction without Considering an Ice-Liquid Interface

The Simultaneous Heat and Water (SHAW) model is a numerical simulation software that is widely used in frozen soil research (Flerchinger and Saxton, 1989). It can simulate water, heat, and solute migration in partially frozen soil. The SHAW model takes into account both heat conduction and water flow, and incorporates the concept of apparent heat capacity to estimate melting phase changes.

$$C\frac{\partial T}{\partial t} - \rho_i L_m \frac{\partial \theta_i}{\partial t} = \frac{\partial}{\partial z}\left[k\frac{\partial T}{\partial z}\right] - \rho_l c_l \frac{\partial q_l T}{\partial z} - L_v\left(\frac{\partial q_v}{\partial z} + \frac{\partial p_v}{\partial t}\right) \quad (2)$$

$$\frac{\partial \theta_l}{\partial t} + \frac{\rho_i}{\rho_l}\frac{\partial \theta_i}{\partial t} = \frac{\partial}{\partial z}\left[K\left(\frac{\partial \psi}{\partial z} + 1\right)\right] + \frac{1}{\rho_l}\frac{\partial q_v}{\partial z} + U \quad (3)$$

In the equations: z denotes soil depth (m); T represents temperature (°C); ρ_i is the ice density (917 kg m^{-3}); ρ_l is the water density (1000 kg m^{-3}); L_m is the latent heat of fusion (3.34×10^5 J kg^{-1}); L_v is the latent heat of vaporization (2.5×10^6 J kg^{-1}); θ_i represents soil ice content (m^3 m^{-3}); θ_l denotes liquid water content (m^3 m^{-3}); c_l is the specific heat capacity of water (4214 J kg^{-1} K^{-1}); q_l represents liquid water flux (m^3 s^{-1}); q_v is the water vapor flux (m^3 s^{-1}); ρ_v represents water vapor density (kg m^{-3}); K denotes the unsaturated hydraulic conductivity (m s^{-1}); Ψ represents soil water potential (m); U is a source/sink term for water flux (m^3 m^{-3} s^{-1}). Recently, He et al. (2021) used the SHAW model to evaluate frozen soil thermal conductivity models. In comparison to studies on phase-change heat conduction (Paterson, 1952; Hahn et al., 2012), the SHAW model approximates the temperatures of the ice and liquid phases as being a single temperature T value (Equation (2). Traditional heat transfer processes under melting conditions involve solving for the temperatures of both ice and liquid phases. The SHAW model also neglects the ice-liquid phase interface during phase transitions. To date, there have been no reports of the model being used to evaluate DPHP measurements on frozen soil.

To explain the deviations of frozen soil DPHP measurements from estimations based on the ILS model, Ochsner and Baker (2008) employed a frozen soil heat transfer model proposed by Fuchs et al. (1978):

$$(C + L_m\rho_l\frac{\partial \theta_l}{\partial T})\frac{\partial T}{\partial t} = \frac{\partial}{\partial z}(k\frac{\partial T}{\partial z} - L_m\rho_l q_l) - q_l C_l\frac{\partial T}{\partial z} \quad (4)$$

where C_l is the heat capacity of liquid water (J m^{-3} K^{-1}).

Similar to the SHAW model, this model does not differentiate between ice and liquid phase temperatures. It approximates the actual phase-change latent heat variation using the concept of apparent heat capacity. Furthermore, neither the SHAW model nor the studies conducted by Fuchs et al. (1978) and Ochsner and Baker (2008) provide an analytical expression for temperature with space and time following a heat pulse input.

2.3. Analytical Solution of Melting Phase Transitions with a Moving Interface in a Cylindrical Coordinate System

The current mainstream DPHP theoretical model (ILS model) does not consider phase transitions, even though ice melting occurs during DPHP measurements (Putkonen, 2003). Once ice melting occurs, the ILS model based on a single-medium heat transfer theory is no longer applicable (Ochsner and Baker, 2008; Liu and Si, 2011). As mentioned in Section 2.2, more complex models that do not differentiate between the ice and liquid phases have unknown accuracy in their estimations. Furthermore, all of these models assume that the soil thermal conductivity remains constant with temperature, which is not realistic (Hansson et al., 2004; Liu and Si, 2011). Therefore, accurate numerical values of temperature under melting conditions are needed as a reference in order to evaluate the accuracy and errors of the ILS model applied to DPHP measurements of frozen soil thermal properties. In this study, we have chosen analytical solutions applicable to ice-liquid phase change heat transfer problems and finite element simulation results as references or standards.

Assuming the presence of ice in a semi-infinite soil with an initial temperature T_i and a phase change temperature T_m ($T_i < T_m$), a line heat source of intensity q' is located at $r = 0$ and releases heat starting from $t > 0$. Assuming that the thermal properties of the ice and liquid phases do not vary with temperature, the temperature evolution of the solid and liquid phases (T) satisfies the following equations (Hahn et al., 2012):

$$\frac{\partial^2 T_l(r,t)}{\partial r^2} = \frac{1}{\alpha_l}\frac{\partial T_l(r,t)}{\partial t} \quad 0 < r < s(t), t > 0 \quad (5)$$

$$\frac{\partial^2 T_s(r,t)}{\partial r^2} = \frac{1}{\alpha_s}\frac{\partial T_s(r,t)}{\partial t} \quad s(t) < r < \infty, t > 0 \quad (6)$$

$$T_s(r \to \infty, t) \to T_i \quad r > 0 \quad (7)$$

$$T_s(r, t = 0) = T_s \quad r > 0 \quad (8)$$

where the subscripts s and l represent the ice and liquid phases, respectively, α_s is the thermal diffusivity of ice (m^2 s^{-1}), and α_l is the thermal diffusivity of liquid water (m^2 s^{-1}). And $s(t)$ denotes the position of the ice-liquid interface.

The temperatures of the solid and liquid phases satisfy the following equation:

$$k_s\frac{\partial T_s}{\partial r} - k_l\frac{\partial T_l}{\partial r} = \rho L_m\frac{ds(t)}{dt} \quad (9)$$

where ρ represents the density (kg m^{-3}).

Paterson (1952) presented the following analytical solution of the heat conduction equation (5), (6)) with the above initial and boundary value problem (Eqs. (7), (8), (9)):

$$T_s = -T_i\left(1 - \frac{Ei\left(-\frac{r^2}{4\alpha_s t}\right)}{Ei\left(-\frac{\delta^2}{4\alpha_s}\right)}\right) \quad (10)$$

$$T_l = \frac{q'}{4\pi k_s}\left(Ei\left(-\frac{\delta^2}{4\alpha_l}\right) - Ei\left(-\frac{r^2}{4\alpha_l t}\right)\right) \quad (11)$$

The position of the solid–liquid interface, $s(t)$, satisfies the following equation:

$$s(t) = \delta\sqrt{t} \quad (12)$$

Table 1
Physical properties of the soil samples used in COMSOL simulations were obtained from the following sources: †He et al. (2015) and ‡Watanabe and Wake (2009).

Soil no.	Soil texture	Soil bulk density (ρ_b) kg m^{-3}	Total water content (θ_T) m^3 m^{-3}
1†	Loamy sand	1690	0.25
2‡	Sand	1430	0.26
3‡	Loam	1045	0.51
4‡	Silt loam	1130	0.37

δ is the root of the following transcendental equation:

$$\frac{q^{‘}}{4\pi}e^{-\delta^2/4\alpha_l}+\frac{k_l(-T_i)}{Ei(-\delta^2/4\alpha_s)}e^{-\delta^2/4\alpha_s}=\delta^2\rho L_m/4 \quad (13)$$

To determine the temperatures on both sides of the liquid water–ice interface in the Paterson (1952) model, the process involves first computing the roots of Equation (13). Subsequently, these calculated roots are substituted into the temperature equations for the solid and liquid phases (Eq. (10) and Eq. (11), respectively). The Paterson (1952) theory differs significantly from the ILS and SHAW models (Flerchinger and Saxton, 1989; He et al., 2021). The Paterson (1952) model can predict the position of the ice-liquid interface and differentiate the temperatures of the solid and liquid phases, while the other models are unable to distinguish between the temperatures of the two phases. To our knowledge, there are no reports of applying the moving boundary heat conduction theory to frozen soil research. However, the Paterson (1952) model assumes that the thermal properties of the soil (thermal conductivity, heat capacity) do not vary with temperature, which contradicts actual frozen soil properties (Hansson et al., 2004; Liu and Si, 2011).

2.4. Computer simulations

Although Paterson (1952) provides an analytical solution for heat transfer between the ice and liquid phases, the theory is not applicable when thermal properties (thermal conductivity, specific heat) vary with temperature. Therefore, we use numerical simulations to model DPHP experiments with temperature-dependent thermal properties. COMSOL Multiphysics (Version 6.0, COMSOL, Inc. Burlington, MA 01803 USA) is used for the simulations. Compared to other numerical simulations (Bao et al., 2016; Flerchinger and Saxton, 1989; He et al., 2021; Zhang et al., 2011), COMSOL Multiphysics offers the following advantages: (1) consideration of realistic ice-liquid phase changes instead of introducing arbitrary parameters such as apparent heat capacity, which lack physical meaning; (2) the ability to separately solve for the temperature distribution ($T(r,t)$) in the frozen (ice) and melted (liquid) regions; (3) the determination of the position of the moving ice-liquid interface.

2.4.1. Simulation Principle

The temperature evolution equations for the ice and liquid phases in the COMSOL simulation are given by equations (5) and (6). The physical properties and parameters of the ice and liquid phases are (COMSOL, 2023)

$$\rho_t=\theta_l\rho_l+\theta_i\rho_i+\rho_b \quad (14)$$

$$C=\frac{1}{\rho_t}(\theta_i\rho_i c_i+\theta_l\rho_l c_l+\rho_b c_s)+L_m\frac{\partial w}{\partial T} \quad (15)$$

$$w=\frac{1}{2}\frac{\theta_l\rho_l-\theta_i\rho_i-\rho_b}{\theta_i\rho_i+\theta_l\rho_l+\rho_b} \quad (16)$$

where ρ_t is the density of the ice-liquid coexistence region, and c_s is the specific heat capacity of the soil minerals (J kg^{-1} K^{-1}). where the subscript i denotes ice. w is the change in the total volume of ice and liquid water.

The soil thermal conductivity value used for the simulations is given by the empirical formula proposed by Hansson et al. (2004):

$$k(\theta_l)=0.55+0.8\left(\theta_l+\left(1+13.05\theta_i^{1.06}\right)\theta_i\right)$$
$$-0.42exp\left\{-\left(3.07\left(\theta_l+\left(1+13.05\theta_i^{1.06}\right)\theta_i\right)\right)^4\right\} \quad (17)$$

2.4.2. Soil parameters

To validate the effectiveness of COMSOL simulations to represent the thermal properties of frozen soil determined by DPHP, we selected the DPHP measurements reported by He et al. (2015) (Fig. 5 in the paper) as a reference. In their study, they measured the soil thermal properties and water content under freezing conditions using DPHP and TDR (time-domain reflectometry) for a loamy sand soil (Table 1).

Watanabe and Wake (2009) measured the liquid water content (θ_l) in partially frozen soils using NMR (nuclear magnetic resonance). We performed COMSOL simulations for the three soils reported by Watanabe and Wake (2009) (Table 1). From these simulations, we obtained optimized heating combinations (heating duration and intensity) for the three soils that minimized the measurement errors in DPHP under freeze–thaw conditions. The bulk density (ρ_b), total water content (θ_T), unfrozen water content (θ_l), and ice content ($\theta_i \approx \theta_T$ - θ_l) parameters were taken from their study.

2.4.3. Simulation approach

We represented DPHP measurements with a two-dimensional cylindrical coordinate system, perpendicular to the axis of the heating needle. This simplification significantly reduced the computational cost by converting the three-dimensional problem into a two-dimensional problem. The COMSOL 2D transient fluid heat transfer module was used to simulate the effect of different heating combinations (cumulative heat intensity $\Delta Q = q^{‘}\,t_0$, heating duration t_0) on the DPHP measurement errors. The specific setup of the COMSOL simulation process was as follows:

(1) The study area is constructed as a square region of 150 mm × 150 mm (Fig. 1), with insulated boundaries. The selected two-dimensional solution domain is sufficiently large ($\gg$ 2.6 r_0) to neglect boundary effects (Campbell et al., 1991). Since the influence of the ice melting phase change can exceed the limited dimensions of the needle (Liu et al., 2011), to further reduce the computational burden, we approximate the DPHP probe with a cylindrical heat source of 0.6 mm in diameter (ignoring the filling material inside the probe and the material of the needle), with a probe spacing of 6 mm.
(2) The material thermal property values are set. Table 2 presents the basic parameters of frozen soil used in the COMSOL simulation. The $\theta_l \sim T$ data for the three soil textures are taken from Watanabe and Wake (2009) (Fig. 2 in their article).
(3) The latent heat of fusion and the temperature range for phase changes are set. Under natural conditions, soil freezing occurs within a broad temperature range below zero degrees Celsius (Li et al., 2019; Overduin et al., 2006). For the simulation results to closely represent real scenarios, we defined the temperature range for liquid-ice phase transitions. Watanabe and Wake (2009) confirmed that major variations in soil ice content (θ_i) primarily occur between temperatures of − 1 °C and 0 °C. Therefore, we set the phase transition temperature range from − 1 °C to 0 °C. Two types of latent heat were considered: a constant value (L_m) corresponding to phase transition at 0 °C, and a variable value ($\Delta\theta_l \times L_m$) corresponding to a specific phase transition range.
(4) Different combinations of T_i, t_0, and ΔQ were evaluated (Table 3, with 9 × 4 × 6 = 216 possible combinations) to determine the

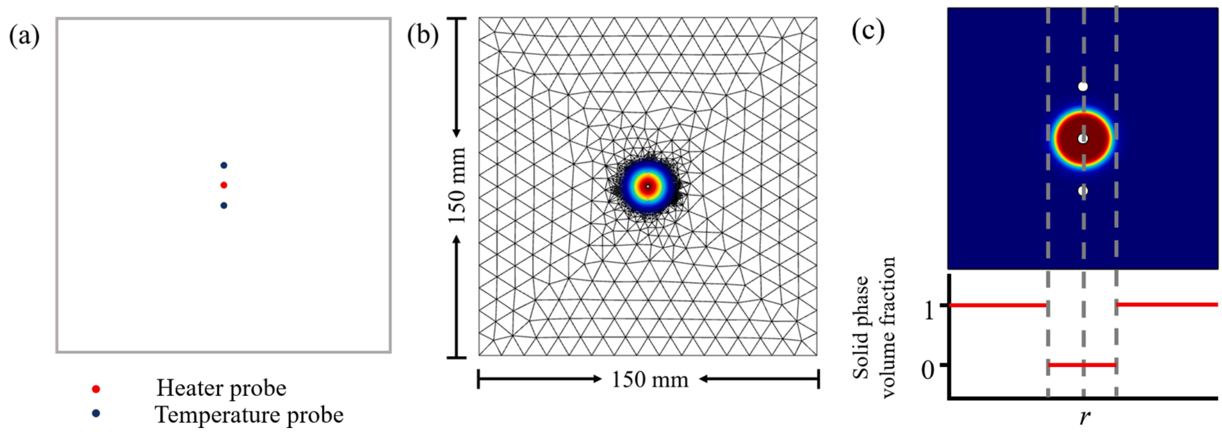

Fig. 1. (a) Schematic diagram of the 2D COMSOL simulation geometry, with the red circle at the center representing the heating needle; (b) Illustrative temperature distribution (in sand, $T_i = -0.25$ °C, $\Delta Q = 1000$ J m^{-1}, $t_0 = 8$ s, $t = 30$ s), using a free triangular mesh; (c) COMSOL simulated distribution of the ice phase (blue area) and liquid phase (red area) around the heater probe at $t = 30$ s (here, the soil and the heating parameters are the same as that of Fig. 1 (b)).

Table 2
Basic physical properties of frozen soil used in the simulations.

Symbols	Numerical value
L_m (J kg^{-1})	[a]3.34×10^5
k_s (W m^{-1} K^{-1})	[b]2.24
k_l (W m^{-1} K^{-1})	[d]0.6
c_i (J kg^{-1} K^{-1})	[c]2030
c_l (J kg^{-1} K^{-1})	[a]4214
ρ_i (kg m^{-3})	[c]917
ρ_l (kg m^{-3})	[d]1000

Note: [a] Kojima et al. (2016); [b] Côté and Konrad. (2005); [c] Liu and Si (2011); [d] He et al. (2015).

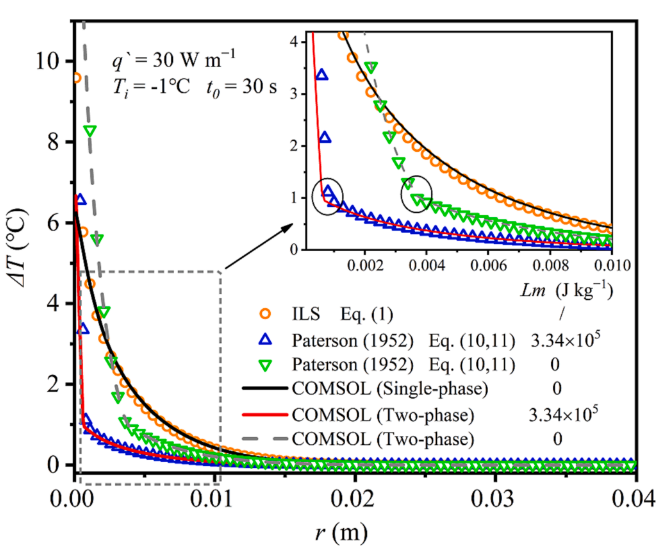

Fig. 2. DPHP radial temperature distributions at $t = 30$ s, from COMSOL simulations, the ILS model, and the analytical solution of Paterson (1952) using ice as the medium. The ILS model, representing single-phase heat transfer, employs $L_m = 0$ J kg^{-1} to denote the latent heat of phase change in the COMSOL simulation.

optimal heating combination (heating duration and cumulative heating intensity) to minimize DPHP measurement errors.

Due to the nonlinear thermal properties of frozen soil (Eq.17), deriving an analytical solution similar to Paterson (1952) is unfeasible.

Table 3
Combinations of heating duration (t_0) and cumulative heating intensity (ΔQ) used for COMSOL simulations.

Parameter	Numerical value
T_i (°C)	−5, −4, −3, −2, −1.5, −1, −0.75, −0.5, − 0.25
t_0 (s)	8, 15, 30, 60
ΔQ (J m^{-1})	200, 400, 600, 800, 1000, 1200

In our COMSOL simulations, equations (5)–(8) were numerically solved using the finite element method. Notably, both the Paterson analytical solution and the COMSOL numerical method share identical sets of partial differential equations, along with their associated initial value problem (IVP) and boundary value problem (BVP). Mathematically, for the same IVP and BVP, there exists a unique corresponding solution. Hence, the difference between them lies solely in the methodology employed: analytical in the case of the Paterson method and numerical in COMSOL simulations. Unlike conventional frozen soil temperature models that rely on single-phase heat conduction (Bao et al., 2016; Flerchinger and Saxton, 1989; Ochsner and Baker, 2008; Zhang et al., 2011), both the COMSOL simulation and the Paterson solution accommodate two-phase heat conduction. Consequently, these two methods enable the generation of transient spatial temperature distributions for both the liquid and solid phases.

3. Results and discussion

3.1. Comparison of COMSOL simulations and ILS model calculations with the Paterson (1952) analytical solution which includes a moving ice-liquid interface

Fig. 2 depicts the COMSOL simulated spatial temperature distribution around the DPHP heating needle at a specific time ($t = 30$ s). Its primary goal is to validate COMSOL's capability to model heat conduction across the moving ice-liquid interface while outlining this interface. Furthermore, it aims to emphasize disparities between models or methodologies that either consider or overlook this pivotal interface. The figure clearly marks the ice-liquid interface with two small black circles. The temperature on the left side of this interface denotes that of liquid water, while the temperature on the right side indicates that of ice. Here, we selected ice as the research medium. By comparing the simulation results, the ILS theory, and the analytical solution proposed by Paterson (1952) (Fig. 2), we also examined the accuracy of COMSOL in the study of thermal properties of frozen soil. From Fig. 2, it can be observed that as the distance r increases at $q' = 30$ W m^{-1}, $t_0 = 30$ s, and

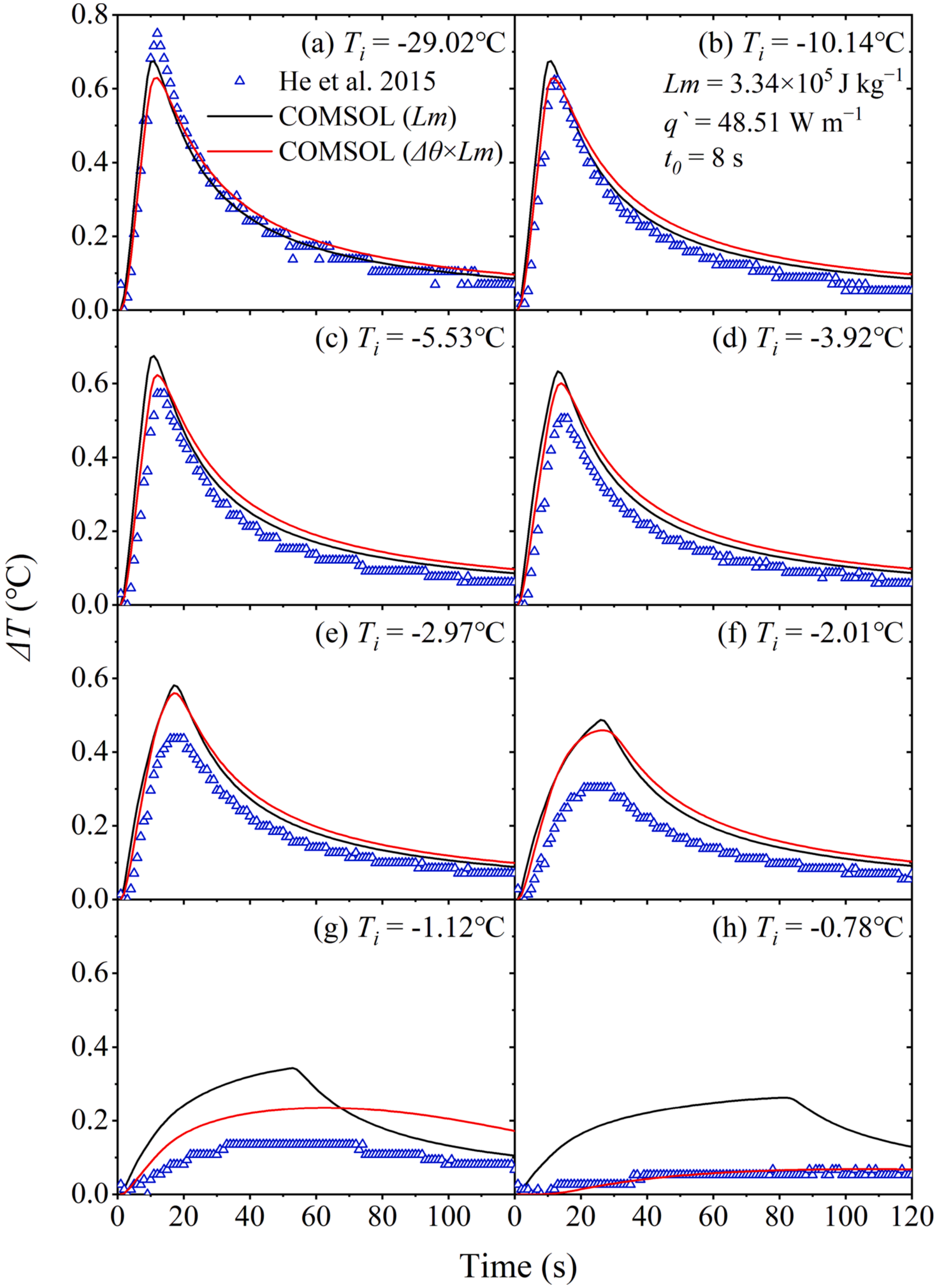

Fig. 3. Comparison of COMSOL simulations with observed temperature values reported by He et al. (2015). Simulations were performed with eight different initial temperatures T_i, while the heating intensity q‘ (48.51 W m^{-1}), and t_0 (8 s) were kept constant. The black curves indicate a phase change temperature of 0 °C and a latent heat, L_m, of (3.34 × 10^5 J kg^{-1}). The red curves indicate that the phase changes occur from − 1 °C to 0 °C, and the latent heat of phase change is $\Delta\theta \times L_m$.

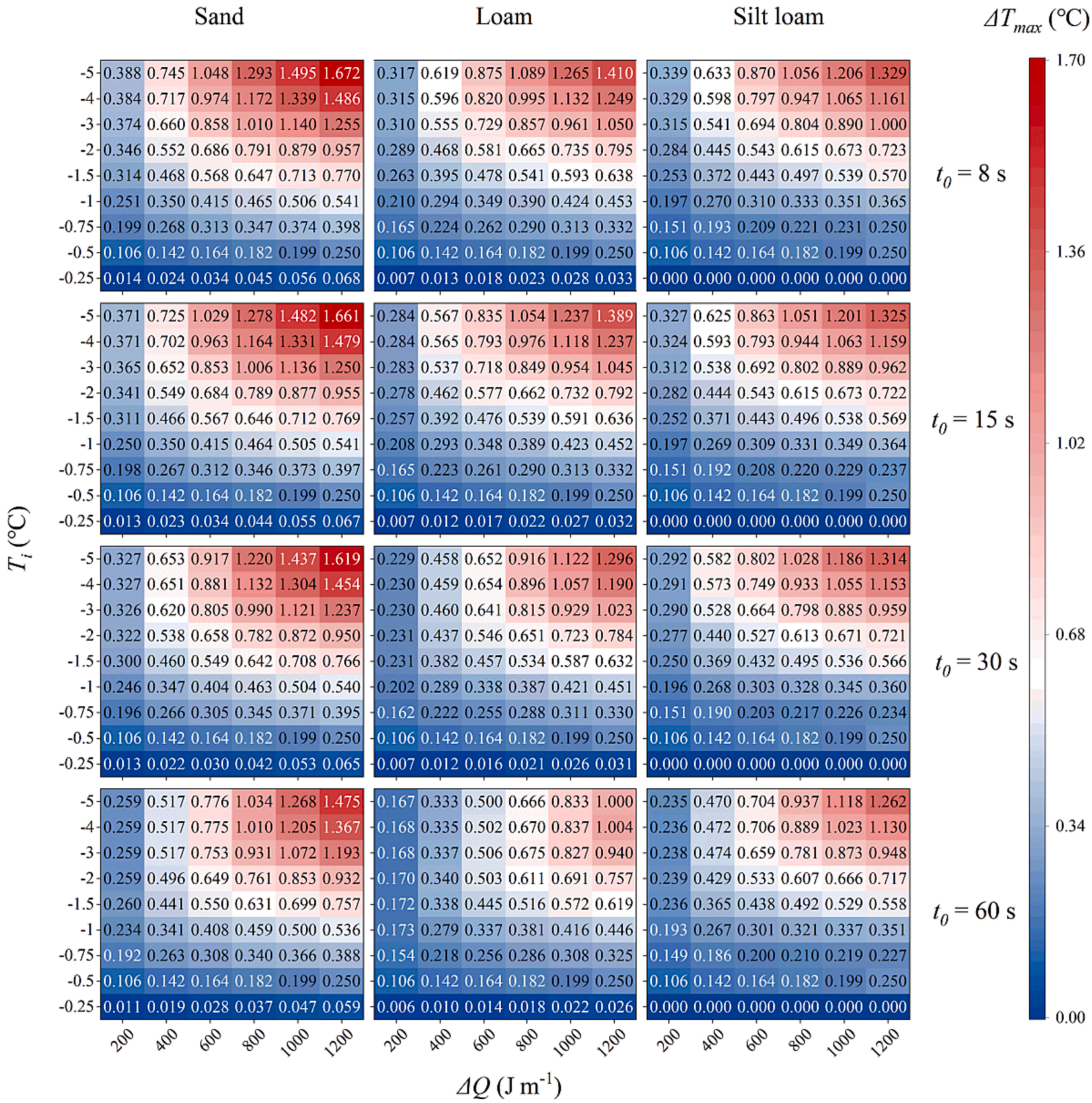

Fig. 4. Simulated maximum temperature change ΔT_{max} (°C) for various DPHP heating combinations (six ΔQ (J/m) and four t_0 (s)) for sand, loam, and silt loam soils (Watanabe and Wake, 2009) at nine selected initial temperatures, T_i, between − 5 °C and − 0.25 °C.

$T_i = -1$ °C, the temperature gradient gradually decreases. During the simulation process, when ice melting is not considered, the COMSOL simulation values (black line, single-phase medium) completely coincide with the ILS model values. When considering ice melting, the simulation results (red line, gray dashed line) coincide with the analytical solution of Paterson (1952) (blue triangles, green inverted triangles). Therefore, COMSOL simulations are able to replicate the ILS theory results and the Paterson (1952) analytical solution results, indicating its applicability to phase-change melting problems.

Fig. 2 also reveals a new phenomenon: when the ice-liquid interface was considered, the spatial temperature distribution significantly differed from the single-phase heat transfer model results (such as the ILS model). This can be seen from the enlarged box indicated by the arrows in Fig. 2. Ignoring the latent heat of phase change, the COMSOL simulation considering the two-phase (solid and liquid, gray dashed line of Fig. 2) and the solution by Paterson (1952) (green inverted triangle) exhibit a perfect match, distinct from both the ILS model (orange circles) and the single-phase simulation (black solid line). These results indicate that when applied to partially frozen soils, the single-phase approximation of the ILS model and other similar models for apparent thermal conductivity and apparent heat capacity (Bao et al., 2016; Flerchinger and Saxton, 1989; Ochsner and Baker, 2008; Zhang et al., 2011) lead to significant systematic errors. This is evident from Fig. 2, where the difference between the green triangles and the solid black line is significant. The ILS solution cannot coincide with the models that consider the ice-liquid interface, because the ILS solution is a smooth continuous function while the models that include the ice-liquid interface are piecewise continuous functions (discontinuous temperature gradient at the solid–liquid or ice-liquid interface). Unlike the ILS model (Eq. (1) and other single-phase approximation models (Eqs. (2)–(4) (Bao et al., 2016; Flerchinger and Saxton, 1989; Ochsner and Baker, 2008; Zhang et al., 2011), which do not account for moving ice-liquid interfaces, both the COMSOL simulations and the Paterson (1952) analytical solution solve the heat conduction equations for solid and liquid phases with moving ice-liquid interfaces (Eqs. (5)–(12)). These methods provide simultaneous spatial temperature distributions for both phases.

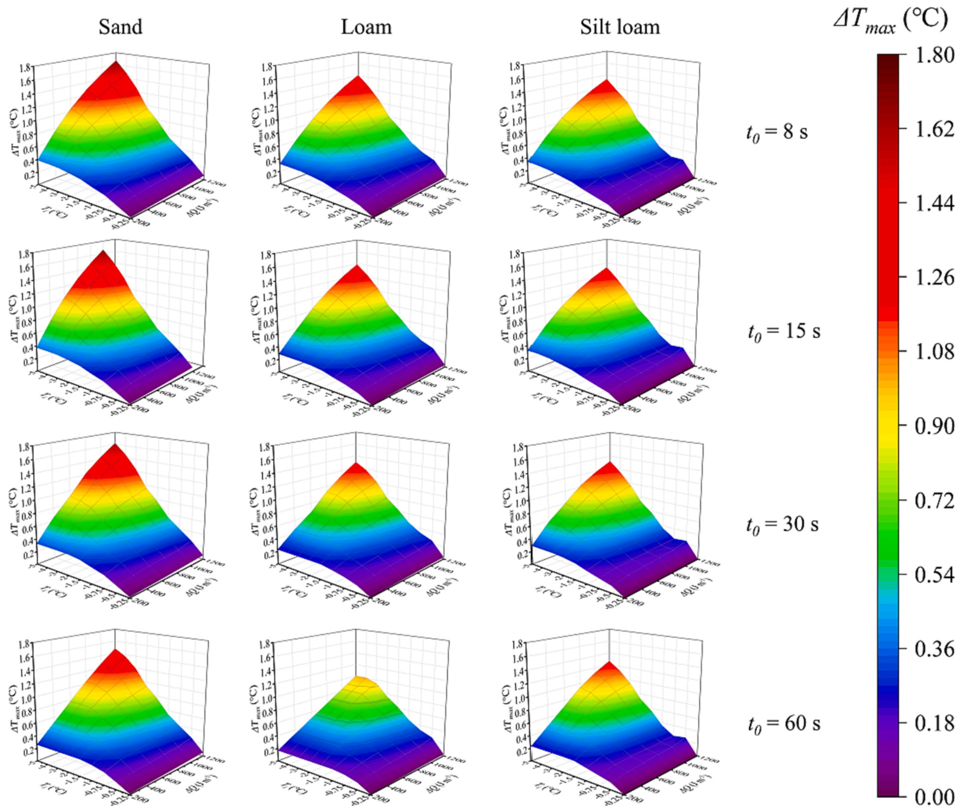

Fig. 5. Simulated 3D contour plots of maximum temperature change ΔT_{max} (°C) for various DPHP heating combinations (six ΔQ (J/m) and four t_0 (s)) at nine different initial temperatures T_i (− 5 °C ∼ − 0.25 °C) for sand, loam, and silt loam soils (Watanabe and Wake, 2009).

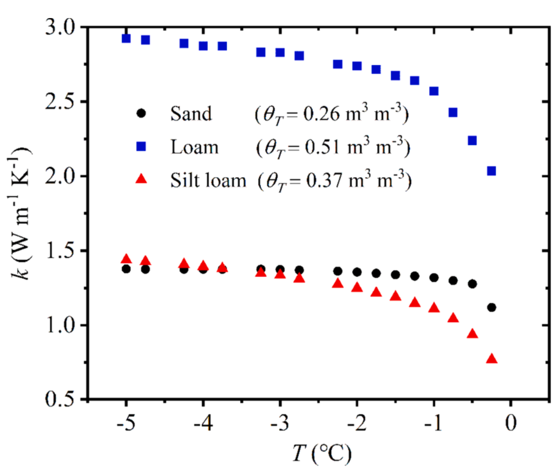

Fig. 6. Soil thermal conductivity k for sand, loam and silt loam of Watanabe and Wake (2009). The values in parentheses are the total water content.

Therefore, to evaluate the inherent errors in the ILS model and other single-phase approximation models (Bao et al., 2016; Flerchinger and Saxton, 1989; Ochsner and Baker, 2008; Zhang et al., 2011), as well as to determine their applicability, comparisons can be drawn using either the results from the COMSOL simulations or the Paterson (1952) solution.

3.2. Comparison of COMSOL simulation results based on the moving ice-liquid interface melting problem to actual frozen soil measurements

In section 3.1, through our study in pure ice, we found that COMSOL simulations, considering and not considering phase-change melting, approximated the predicted results of Paterson (1952) and the ILS model, respectively. Here, we further examine the feasibility of using COMSOL simulations for DPHP measurements in actual frozen soils. We compare the simulation results with the results from actual experiments performed on frozen soils (Brightbank loamy sand from He et al., 2015). The results (Fig. 3) demonstrate that by setting the interval of phase-change occurrence and considering the latent heat of phase-change in the COMSOL simulation, we can essentially reproduce the DPHP results from frozen soils. From Fig. 3, it can be observed that the simulation results exhibit trends similar to the measurements. The response curves of the temperature probes sharpen as the initial temperature of the soil decreases (Fig. 3a, b, c). When the initial temperature approaches 0 °C, the maximum temperature rise decreases, and the peak of the temperature rise becomes gentle and flat (Fig. 3f, g, h). This is consistent with the measured results reported by Ochsner and Baker (2008). At − 0.78 °C, the temperature continues to rise without a peak (Fig. 3h). This may be due to the fact that as the temperature approaches 0 °C, the ice in partially frozen soil is especially prone to melting. At this point, the heat released by a DPHP sensor is not only used to raise the local soil temperature but also utilized for the phase-change (i.e melting) process.

The black curves in Fig. 3 (phase-change occurring at 0 °C) show that the simulated and observed values are in good agreement when the initial temperature is below − 5.5 °C. However, when the initial temperature is in the range of − 5.5 °C to 0 °C, the simulated results are significantly larger than the observed values. This discrepancy may be attributed to the assumption of phase-changes occurring at 0 °C. In actual soil, ice starts to melt when the temperature is below 0 °C (Overduin et al., 2006). This means that below 0 °C, both liquid water and ice coexist in the partially frozen soil (Li et al., 2019; Overduin et al., 2006; Zhang et al., 2011; Zhang et al., 2018). Additionally, in some of our COMSOL simulations, we set L_m as a constant value (Fig. 3, black curve), which does not match the actual situation. In actual frozen soil, the latent heat of phase-change is a function of temperature (Bao et al., 2016). Measurements by He et al. (2015) show that the maximum

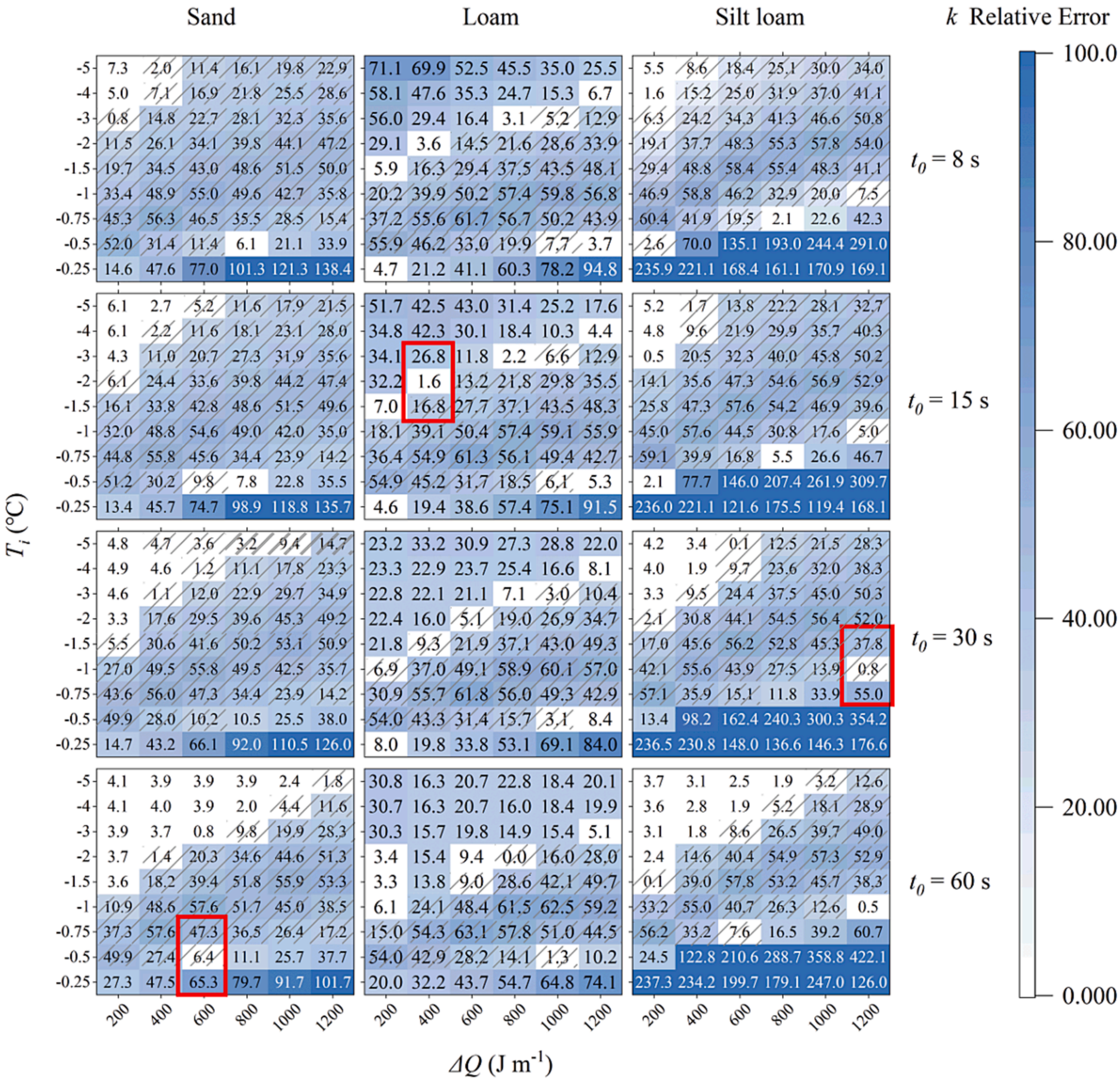

Fig. 7. Relative errors of DPHP determined k values for sand, loam, and silt loam, based on COMSOL simulated values. The simulations were performed for various T_i, ΔQ and t_0. Soil thermal property values, liquid water content and ice content were obtained from Watanabe and Wake (2009). (Note: The black diagonal lines marked with squares in the figure represent negative relative errors, indicating underestimations of the true values estimated by the ILS model). The red boxed areas correspond to the occurrence of U-shaped reversals in thermal conductivity error when temperature undergoes continuous variations. For a more detailed analysis and explanation, please refer to Fig. 9.

amount of DPHP heat pulse induced ice melting occurred in the temperature range of − 1.5 °C to − 0.5 °C. Both C and L_m change rapidly with temperature within this range. Therefore, to consider pre-melting, we set the phase-change temperature for ice melting to − 1.5 °C to − 0.5 °C (a range of 1 °C where phase-change occurs). By calculating the variation of latent heat with temperature using $\Delta\theta_l \times L_m$, the improved simulation results are shown by the red curves in Fig. 3.

Compared to the black curves, the red curves in Fig. 3 better agree with the measured values when the initial temperature is larger than − 2.0 °C (RMSE < 0.095 °C). However, at initial temperatures of − 3.0 °C, −2.0 °C, and − 1.1 °C, the simulated values are larger than the measured values. This discrepancy may be due in part to TDR measurement errors of the liquid water content (He et al., 2015). Tian et al. (2015) report that the freezing of pore water in wet soil can cause soil expansion, which affects the accuracy of TDR measurements. Additionally, factors such as the length of the TDR probe and the spacing between probes can influence the accuracy of TDR measurements (Heimovaara, 1993; Knight, 1992). Another potential explanation for the difference between simulated and measured temperatures could stem from overlooking the thermal properties of the stainless steel needles (Knight et al., 2012) filled with epoxy. Particularly, when temperature changes are small, the impact of thermal disequilibrium among soil water, ice, and probe needles might become more pronounced. It is important to note that curve-fitted results are not presented in Fig. 3. Although the simulated values (red curves in Fig. 3) do not perfectly match the measurements, the overall trends of the two are very close. This indicates that COMSOL simulations of DPHP measurements in frozen soil can provide reliable results.

3.3. Optimization of heating parameters (cumulative heat intensity and heating duration) for DPHP frozen soil measurements based on COMSOL simulations

Information presented in Figs. 2 and 3 validates the accuracy and

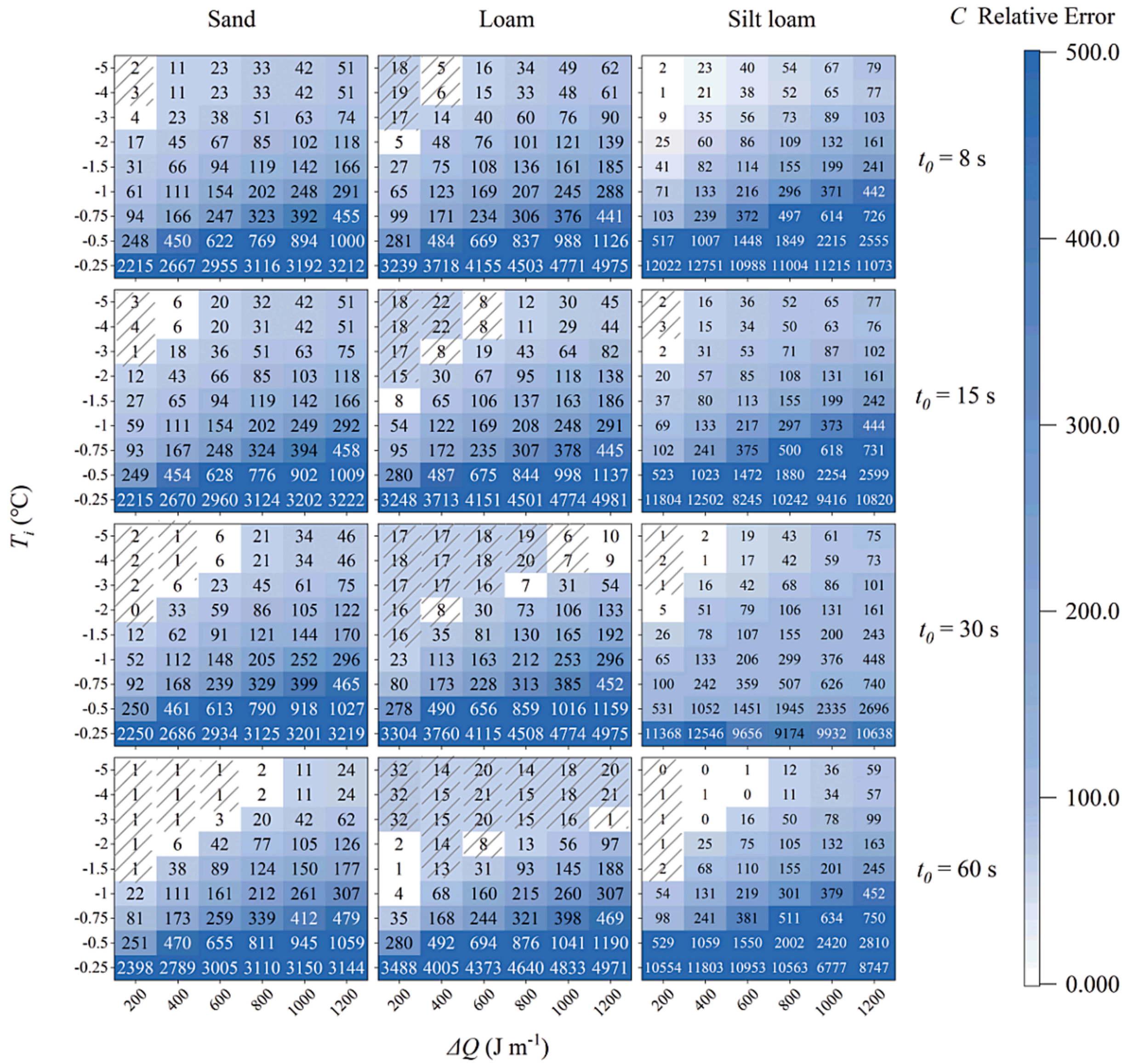

Fig. 8. Relative errors of DPHP determined *C* values for sand, loam, and silt loam, based on COMSOL simulated values. Sand, loam, and silt loam soils from Watanabe and Wake (2009) were used for the simulations. (Note: The black diagonal lines marked with squares in the figure represent negative relative errors, indicating underestimations of the true values by the ILS model).

reliability of COMSOL simulations of DPHP measurements in frozen soil. In Figs. 4 and 5, we utilize COMSOL simulations to evaluate the use of a DPHP sensor in three soils with various textures (the soil thermal property values are referenced in Table 1). A total of 216 combinations are studied for each soil texture ($-5\ ^\circ C < T_i < 0\ ^\circ C$, $200 < \Delta Q < 1200$ J m^{-1}, 8 s $< t_0 <$ 60 s). The maximum temperature increase (ΔT_{max}) in response to a heat pulse is used to calculate soil thermal conductivity (k) (Bristow et al., 1993). Large ΔT_{max} values indicate significant temperature rises near the heating probe, which can result in large errors if the ILS model is used without considering phase changes. Therefore, we select ΔT_{max} to qualitatively analyze the influence of ΔQ and t_0 on DPHP measurements. Fig. 4 displays the ΔT_{max} values for various heat input combinations to the three soils. The trends exhibited by the three soils are generally similar for the various combinations of t_0 and ΔQ, ΔT_{max} increases with increasing ΔQ. For fixed T_i and ΔQ values, a longer t_0 produces smaller ΔT_{max} indicating a lower degree of melting near the heating probe. These results confirm the Liu and Si (2011) suggestion that measurement errors can be reduced by increasing t_0. In general, sand (Fig. 4) has larger ΔT_{max} values than loam and silt loam soils. For fixed t_0 and ΔQ values, soil with lower T_i produces larger ΔT_{max} because lower temperatures result in less melting induced by the heating probe. Fig. 5 presents a graphical depiction of the numbers presented in Fig. 4. The patterns among the optimized heating combinations can be observed in Fig. 5.

The qualitative analysis discussed above regarding ΔT_{max} can only provide an indication of the ease of melting induced by different heating combinations, but it fails to quantify the measurement error of the DPHP method. Currently, there is a lack of analytical solutions for the thermal conduction equation in frozen soil with temperature dependent thermal properties (Hahn et al., 2012), making it difficult to obtain accurate thermal properties from DPHP experiments by curve fitting. This leads to a lack of reference values for the thermal properties in existing DPHP studies on frozen soil (Liu and Si, 2011; Kojima et al., 2016; Kojima et al., 2018), which hinders the evaluation of measurement errors in DPHP-based thermal property measurements (Putkonen, 2003). The results presented in Figs. 2 and 3 demonstrate the close agreement between COMSOL simulations and frozen soil DPHP measurements. In the following analysis, we utilize COMSOL simulations to provide an

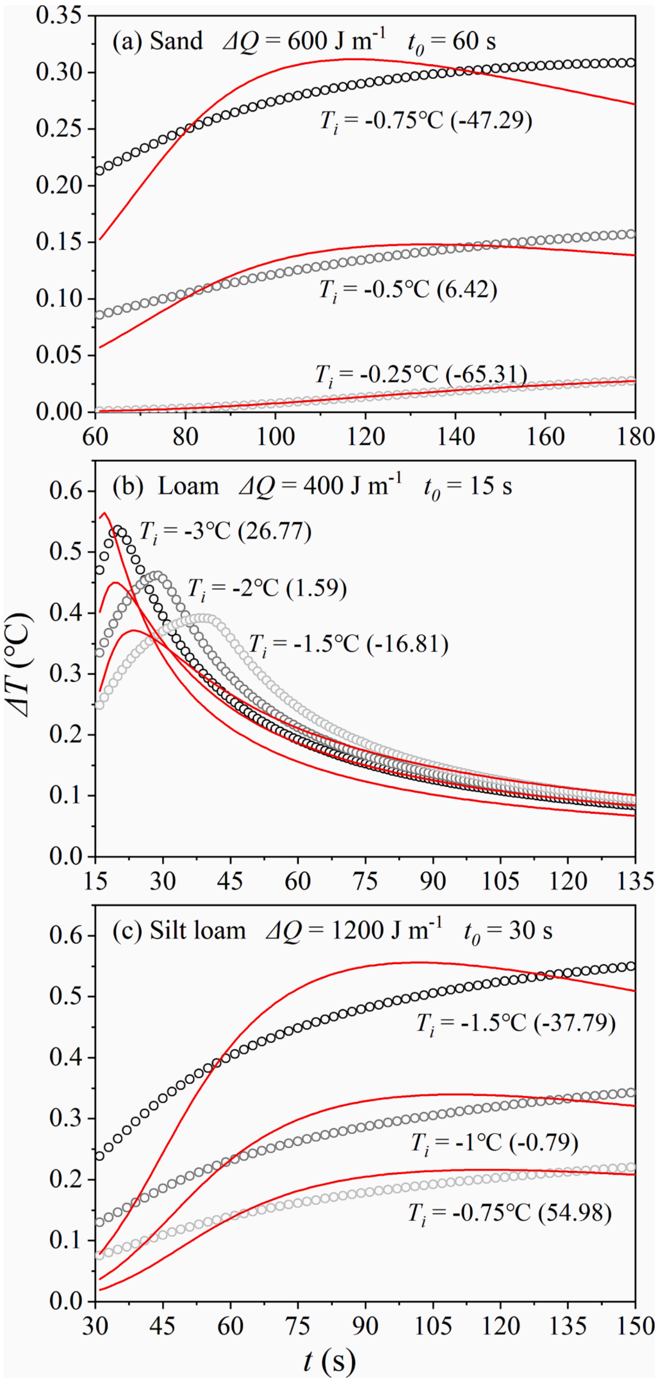

Fig. 9. COMSOL simulations (symbols) for sand, loam and silt loam soils and the fitted ILS curves (red curves). The values in parentheses are the relative error of *k*. Here, the curves representing the three soil simulations correspond to the temperatures marked within the red-boxed area in Fig. 7.

estimation of the measurement error in DPHP-based thermal property measurements of frozen soil.

Figs. 7 and 8 depict the relative errors of thermal conductivity (*k*) and heat capacity (*C*) for the three different soils under various heating combinations. Overall, both *k* and *C* exhibit similar error trends, with decreasing errors for increasing heating duration under a fixed cumulative heating intensity. This finding is consistent with the observations of Liu and Si (2011), although their measurements were performed on coarse sand with a particle size of 2 mm and fine sand with a particle size of 0.4 mm. Similar reports of reducing measurement errors by extending the heating duration have also been reported by He et al. (2015). The agreement between simulated and measured results in terms of trends further demonstrates that COMSOL simulations, with reliable soil thermal property input data, can reproduce DPHP measurements in frozen soils. Similar to the conclusions drawn from Figures 4 and 5, higher ΔT_{max} values corresponding to the same T_i and t_0 result in larger errors in thermal properties. Therefore, when the initial temperature is < -1 °C, controlling the heating duration and intensity can effectively mitigate DPHP measurement errors in frozen soils.

It is worth noting that the error plots (Figs. 7 and 8) do not exhibit clear trends like those in the contour plots of ΔT_{max} (Figs. 4 and 5) (with many randomly distributed white regions in both Fig. 7 and Fig. 8). This discrepancy is attributed to the assumptions of the ILS model. The model assumes single-phase heat conduction, whereas actual partially frozen soil has both ice and liquid phases. Therefore, extracting soil thermal property values by fitting the ILS model to DPHP heat pulse induced temperature with time data introduces significant errors. As demonstrated in Fig. 2, the differences between the ILS model, the Paterson analytical solution considering phase change, and the COMSOL simulation leads to an imperfect overlap (Fig. 9 except for $T_i = -0.25$ °C) of the ILS model and the simulation estimates. It should be noted that the degree of agreement between the simulations and the ILS model should not be used to determine the magnitude of the error. For example, in Fig. 9a, although the simulation results perfectly match the ILS model at $T_i = -0.25$ °C, the error in k actually decreases as T_i changes from -0.25 °C to -0.5 °C. The random characteristics observed in the white regions of Figs. 7 and 8 may be related to the temperature (and liquid water content) dependency of frozen soil conductivity (Fig. 6). This results in the traditional linear heat conduction equation of DPHP theory (De Vries, 1952; Kluitenberg et al., 1995) becoming a nonlinear partial differential equation. Furthermore, the phase change and the corresponding ice-liquid moving interface (Eq. (10)–(13) further nonlinearize the DPHP temperature response. The combined effect of these nonlinear factors leads to the generation of random errors in fitting the ILS model based on linear heat conduction theory to observed temperature with time values (Figs. 7 and 8).

Considering that the ILS model does not account for the latent heat of ice melting, it is not a surprise to discover that, for initial temperatures ranging from -0.5 °C to 0 °C, the relative error in ILS model estimates of *k* is greater than 100 %. Thus, within this temperature range, it is necessary to analyze DPHP measurements with analytical solutions and models (Eq. (10)–(11) that consider the melting phase change. To mitigate the impact of ice melting, it is crucial to select appropriate DPHP heating parameters. For sand, loam, and silt loam soils, we recommend using $200 < \Delta Q < 400$ J m^{-1} when 8 s $< t_0 <$ 60 s. For loam soil with $t_0 = 60$ s, $\Delta Q = 800$ J m^{-1} should be used. For silt loam soil with $t_0 = 60$ s, we recommend using $\Delta Q = 600$ J m^{-1}. If the ILS model is used to estimate soil thermal property values, we recommend using $200 < \Delta Q < 600$ J m^{-1} and 30 s $< t_0 <$ 60 s for sand and silt loam soils. For loam soil, we recommend using $400 < \Delta Q < 800$ J m^{-1} and 30 s $< t_0 <$ 60 s.

Our COMSOL simulations have some limitations. For example, they neglect fluctuations in the ambient background temperature (Jury and Bellantuoni, 1976; Sang et al., 2021) and do not consider the finite size of the DPHP sensor needles (Knight et al., 2016; Liu et al., 2011). The thermal property values of selected frozen soils are based on either DPHP measurements (He et al., 2015) or an empirical model (Hansson et al., 2004) These thermal property values themselves contain errors, which are then propagated into the COMSOL simulation results. Furthermore, the simulation study only includes three types of frozen soil, so the generalizability of the findings requires further investigation.

4. Conclusions

The measurement of frozen soil thermal property values is crucial for engineering construction and agricultural activity. Currently, there is a lack of theory applicable to the use of DPHP sensors in frozen soil, which makes it impossible to evaluate DPHP frozen soil measurement errors. For DPHP frozen soil measurements, we use the COMSOL transient heat transfer module for simulations to study heat transfer with a moving ice-liquid interface. We also compared the COMSOL simulations to the Paterson (1952) analytical solution, the ILS model, and DPHP sensor measurements in frozen soil. The results indicate that, if there is no phase change, the COMSOL simulation agrees perfectly with the ILS model. When thermal property values are temperature independent, the COMSOL simulation results are in full agreement with the results of the analytical solution of Paterson (1952). Thus, COMSOL simulations can effectively deal with transient melting phase changes during heat conduction. The presence of an ice-liquid moving interface renders ineffective the ILS model based on single-phase heat transfer. COMSOL simulations based on actual frozen soil experiments of He et al. (2015) are in good agreement with the measured values. Finally, we performed simulations for the three frozen soils of Watanabe and Wake (2009), and determined the optimal heating combinations to reduce thermal property measurement errors. The results based on ΔT_{max} show that using ΔQ of 200 to 400 J m^{-1} and t_0 of 8 s to 60 s in sand, loam and silt loam soils can effectively reduce the errors due to ice melting. Based on error analysis for the ILS model, we recommend using $200 < \Delta Q < 600$ J m^{-1} and 30 s $< t_0 <$ 60 s for sand and silt loam soils, and $400 < \Delta Q < 800$ J m^{-1} and 30 s $< t_0 <$ 60 s for loam soil.

CRediT authorship contribution statement

Tianyue Zhao: Methodology, Software, Validation, Writing – original draft. **Yuanyuan Zhang:** Formal analysis, Methodology, Software, Validation, Writing – original draft. **Hailong He:** Data curation, Investigation, Resources. **Robert Horton:** Formal analysis, Methodology, Writing – review & editing. **Gang Liu:** Conceptualization, Methodology, Project administration, Software, Supervision, Writing – original draft, Writing – review & editing.

Declaration of competing interest

The authors declare that they have no known competing financial interests or personal relationships that could have appeared to influence the work reported in this paper.

Data availability

The data that has been used is confidential.

Acknowledgements

This work was supported by the Natural Science Foundation of China (Grant No. 42077008 and Grant No. 41771257), the USA National Science Foundation (Grant No. 2037504), and USDA-NIFA Multi-State Project 4188.

References

Arfken, G.B., Weber, H.J., 2005. Mathematical methods for physicists, 6th ed. Elsevier, Amsterdam; Boston. by George B. Arfken and Hans J. Weber. Published:

Bao, H., Koike, T., Yang, K., Wang, L., Shrestha, M., Lawford, P., 2016. Development of an enthalpy-based frozen soil model and its validation in a cold region in China. J. Geophys. Res. Atmos. 121, 5259–5280. https://doi.org/10.1002/2015JD024451.

Bristow, K.L., Horton, R., Kluitenberg, G.J., 1994. Measurement of soil thermal properties with a dual-probe heat-pulse technique. Soil Sci. Soc. Am. J. 58, 1288–1294. https://doi.org/10.2136/sssaj1994.03615995005800050002x.

Cuo, L., Zhao, H., Zhang, Y., Li, N., Liang, L., Liu, Z., Ding, J., Zhu, F., 2023. Spatiotemporally heterogeneous soil thermohydraulic processes in the frozen soil of the Tibetan Plateau. Geoderma 438, 116634. https://doi.org/10.1016/j.geoderma.2023.116634.

De Vries, D.A., 1963. Thermal properties of soil. In: van Dijk, W.R. (Ed.), Physics of Plant Environment. North Holland Publishing, Amsterdam, pp. 210–235.

Flerchinger, G., Saxton, K., 1989. Simultaneous Heat and Water Model of a Freezing Snow-Residue-Soil System II. Transactions of the ASAE 32, 0573–0576. https://doi.org/10.13031/2013.31041.

Fuchs, M., Campbell, G.S., Papendick, R.I., 1978. An Analysis of Sensible and Latent Heat Flow in a Partially Frozen Unsaturated Soil. Soil Sci. Soc. Am. J. 42, 379–385. https://doi.org/10.2136/sssaj1978.03615995004200030001x.

Hahn, D.W., Özisik, M.N., 2012. Heat conduction. John Wiley & Sons.

Hansson, K., Simunek, J., Mizoguchi, M., Lundin, L.-C., van Genuchten, M.T., 2004. Water flow and heat transport in frozen soil: Numerical solution and freeze-thaw applications. Vadose Zone J. 3, 693–704. https://doi.org/10.2113/3.2.693.

He, H., Dyck, M., Wang, J., Lv, J., 2015. Evaluation of TDR for Quantifying Heat-Pulse-Method-Induced Ice Melting in Frozen Soils. Soil Sci. Soc. Am. J. 79, 1275–1288. https://doi.org/10.2136/sssaj2014.12.0499.

He, H., Flerchinger, G.N., Kojima, Y., Dyck, M., Lv, J., 2020. A review and evaluation of 39 thermal conductivity models for frozen soils. Geoderma 382, 114694. https://doi.org/10.1016/j.geoderma.2020.114694.

He, H., Flerchinger, G., Kojima, Y., He, D., Hardegree, S., Dyck, M., Horton, R., Wu, Q., Si, B., Lv, J., Wang, J., 2021. Evaluation of 14 frozen soil thermal conductivity models with observations and SHAW model simulations. Geoderma 403, 115207. https://doi.org/10.1016/j.geoderma.2021.115207.

Heimovaara, T.J., 1993. Design of Triple-Wire Time Domain Reflectometry Probes in Practice and Theory. Soil Sci. Soc. Am. J. 57, 1410–1417. https://doi.org/10.2136/sssaj1993.03615995005700060003x.

Jury, W.A., Bellantuoni, B., 1976. A Background Temperature Correction for Thermal Conductivity Probes. Soil Sci. Soc. Am. J. 40, 608–610. https://doi.org/10.2136/sssaj1976.03615995004000040040x.

Kluitenberg, G.J., Ham, J.M., Bristow, K.L., 1993. Error Analysis of the Heat Pulse Method for Measuring Soil Volumetric Heat Capacity. Soil Sci. Soc. Am. J. 57, 1444–1451. https://doi.org/10.2136/sssaj1993.03615995005700060008x.

Kluitenberg, G.J., Bristow, K.L., Das, B.S., 1995. Error Analysis of Heat Pulse Method for Measuring Soil Heat Capacity, Diffusivity, and Conductivity. Soil Sci. Soc. Am. J. 59, 719–726. https://doi.org/10.2136/sssaj1995.03615995005900030013x.

Knight, J.H., 1992. Sensitivity of time domain reflectometry measurements to lateral variations in soil water content. Water Resour. Res. 28, 2345–2352. https://doi.org/10.1029/92WR00747.

COMSOL, 2023. Comsol application library. Phase Change Models. https://www.comsol.com/model/phase-change-474 (Retrieved December 4, 2023).

Knight J H, Kluitenberg G J, Kamai T, et al. Semianalytical solution for dual-probe heat-pulse applications that accounts for probe radius and heat capacity[J]. Vadose Zone Journal, 2012, 11(2).Knight, J.H., Kluitenberg, G.J., Kamai, T. 2016. The dual probe heat pulse method: interaction between probes of finite radius and finite heat capacity. *Journal of Engineering Mathematics*, **99,** 79-102.https://doi.org/10.1007/s10665-015-9822-x.

Kojima, Y., Heitman, J.L., Flerchinger, G.N., Ren, T., Horton, R. 2016. Sensible Heat Balance Estimates of Transient Soil Ice Contents. *Vadose Zone Journal*, **15,** vzj2015.2010.0134.https://doi.org/10.2136/vzj2015.10.0134.

Kojima, Y., Heitman, J.L., Noborio, K., Ren, T., Horton, R., 2018. Sensitivity analysis of temperature changes for determining thermal properties of partially frozen soil with a dual probe heat pulse sensor. Cold Reg. Sci. Technol. 151, 188–195. https://doi.org/10.1016/j.coldregions.2018.03.022.

Li, S., Wang, C., Shi, L., Yin, N., 2019. Statistical characteristics of the thermal conductivity of frozen clay at different water contents. Results Phys. 13, 102179 https://doi.org/10.1016/j.rinp.2019.102179.

Liu, G., Li, B.G., Hu, K.L., van Genuchten, M.T., 2006. Simulating the gas diffusion coefficient in macropore network images: Influence of soil pore morphology. Soil Sci. Soc. Am. J. 70, 1252–1261. https://doi.org/10.2136/sssaj2005.0199.

Liu, G., Li, B., Ren, T., Horton, R., Si, B.C., 2008. Analytical Solution of Heat Pulse Method in a Parallelepiped Sample Space with Inclined Needles. Soil Sci. Soc. Am. J. 72, 1208–1216. https://doi.org/10.2136/sssaj2007.0260.

Liu, G.C., Si, B., 2011. Soil ice content measurement using a heat pulse probe method. Can. J. Soil Sci. 91, 235–246. https://doi.org/10.4141/cjss09120.

Liu, G., Wen, M.M., Ren, R.Q., Si, B., Horton, R., Hu, K.L., 2016. A general in situ probe spacing correction method for dual probe heat pulse sensor. Agric. For. Meteorol. 226, 50–56. https://doi.org/10.1016/j.agrformet.2016.05.011.

Mustamo, P., Ronkanen, A.K., Berglund, Ö., Berglund, K., Kløve, B., 2019. Thermal conductivity of unfrozen and partially frozen managed peat soils. Soil Tillage Res. 191, 245–255. https://doi.org/10.1016/j.still.2019.02.017.

Ochsner, T.E., Baker, J.M., 2008. In Situ Monitoring of Soil Thermal Properties and Heat Flux during Freezing and Thawing. 72, 1025–1032. https://doi.org/10.2136/sssaj2007.0283.

Orakoglu Firat, M.E., Atila, O., 2021. Investigation of the thermal conductivity of soil subjected to freeze-thaw cycles using the artificial neural network model. Calorimetry Journal of Thermal Analysis and. https://doi.org/10.1007/s10973-021-11081-x.

Overduin, P.P., Kane, D.L., van Loon, W.K.P., 2006. Measuring thermal conductivity in freezing and thawing soil using the soil temperature response to heating. Cold Reg. Sci. Technol. 45, 8–22. https://doi.org/10.1016/j.coldregions.2005.12.003.

Paterson, S., 1952. Propagation of a Boundary of Fusion. Glasg. Math. J. 1, 42–47. https://doi.org/10.1017/S2040618500032937.

Putkonen, J., 2003. Determination of frozen soil thermal properties by heated needle probe. Frozen Soil and Periglacial Processes 14, 343–347. https://doi.org/10.1002/ppp.465.

Rooney, E.C., Bailey, V.L., Patel, K.F., Dragila, M., Battu, A.K., Buchko, A.C., Gallo, A.C., Hatten, J., Possinger, A.R., Qafoku, O., Reno, L.R., SanClements, M., Varga, T., Lybrand, R.A., 2022. Soil pore network response to freeze-thaw cycles in frozen soil aggregates. Geoderma 411, 11. https://doi.org/10.1016/j.geoderma.2021.115674.

Sang, Y.J., Liu, G., Horton, R., 2020. Wind effects on soil thermal properties measured by the dual-probe heat pulse method. Soil Sci. Soc. Am. J. 84, 414–424. https://doi.org/10.1002/saj2.20041.

Sang, Y.J., Liu, G., Ren, T.S., 2021. Field test of two background temperature correction methods of dual probe heat pulse method. Geoderma 401, 115349. https://doi.org/10.1016/j.geoderma.2021.115349.

Tian, Z., Heitman, J., Horton, R., Ren, T. 2015. Determining Soil Ice Contents during Freezing and Thawing with Thermo-Time Domain Reflectometry. *Vadose Zone Journal*, **14,** vzj2014.2012.0179.https://doi.org/10.2136/vzj2014.12.0179.

Watanabe, K., Wake, T., 2009. Measurement of unfrozen water content and relative permittivity of frozen unsaturated soil using NMR and TDR. Cold Reg. Sci. Technol. 59, 34–41. https://doi.org/10.1016/j.coldregions.2009.05.011.

Zhang, M., Lu, J., Lai, Y., Zhang, X., 2018. Variation of the thermal conductivity of a silty clay during a freezing-thawing process. Int. J. Heat Mass Transf. 124, 1059–1067. https://doi.org/10.1016/j.ijheatmasstransfer.2018.02.118.

Zhang, Y., Treberg, M., Carey, S.K., 2011. Evaluation of the heat pulse probe method for determining frozen soil moisture content. Water Resour. Res. 47, W05544. https://doi.org/10.1029/2010WR010085.

Zhao, Y., Si, B., 2018. Thermal properties of sandy and peat soils under unfrozen and frozen conditions. Soil Tillage Res. 189, 64–72. https://doi.org/10.1016/j.still.2018.12.026.

Zhao, X., Zhou, G., Jiang, X., 2019. Measurement of thermal conductivity for frozen soil at temperatures close to 0 °C. Measurement 140, 504–510. https://doi.org/10.1016/j.measurement.2019.03.069.